Isolation and Characterization of Fission Yeast sns Mutants Defective at the Mitosis-to-Interphase Transition

Anna Matynia,† Ulrich Mueller,* Ngoctuyen Ong,* Janos Demeter,* Aaron L. Granger,* Kaede Hinata* and Shelley Sazer*,†

**Verna and Marrs McLean Department of Biochemistry and †Department of Cell Biology, Baylor College of Medicine, Houston, Texas 77030*

Manuscript received June 30, 1997
Accepted for publication January 5, 1998

ABSTRACT

pim1-d1^{ts} was previously identified in a visual screen for fission yeast mutants unable to complete the mitosis-to-interphase transition. *pim1*$^{+}$ encodes the guanine nucleotide exchange factor (GEF) for the spi1 GTPase. Perturbations of this GTPase system by either mutation or overproduction of its regulatory proteins cause cells to arrest with postmitotic condensed chromosomes, an unreplicated genome, and a wide medial septum. The septation phenotype of pim1-d1^{ts} was used as the basis for a more extensive screen for this novel class of sns (septated, not in S-phase) mutants. Seventeen mutants representing 14 complementation groups were isolated. Three strains, sns-A3, sns-A5, and sns-A6, representing two different alleles, are mutated in the *pim1*$^{+}$ gene. Of the 13 non-*pim1*^{ts} sns complementation groups, 11 showed genetic interactions with the spi1 GTPase system. The genes mutated in 10 sns strains were synthetically lethal with *pim1-d1*, and six sns strains were hypersensitive to overexpression of one or more of the known components of the spi1 GTPase system. Epistasis analysis places the action of the genes mutated in nine of these strains downstream of *pim1*$^{+}$ and the action of one gene upstream of *pim1*$^{+}$. Three strains, sns-A2, sns-B1, and sns-B9, showed genetic interaction with the spi1 GTPase system in every test performed. sns-B1 and sns-B9 are likely to identify downstream targets, whereas sns-A2 is likely to identify upstream regulators of the spi1 GTPase system that are required for the mitosis-to-interphase transition.

AT the mitosis-to-interphase transition in yeast cells, the chromosomes decondense, the mitotic spindle is disassembled and the cytoplasmic microtubule array is reassembled, and the single nuclear envelope, which remains intact during mitosis, is resolved into two individual nuclear envelopes surrounding the chromatin (Hagan and Hyams 1988; Robinow and Hyams 1989). Although these structural changes have been well documented, very little is known about their regulation and coordination.

The identification and characterization of budding and fission yeast mutants that are unable to execute particular steps in the cell cycle and the subsequent cloning of the genes mutated in these strains have provided critical information about cell cycle regulatory proteins (Murray and Hunt 1993). The original screen for fission yeast cell division cycle mutants was designed based on the observation that progression through the cell cycle could be separated from cell growth (Nurse 1975; Nasmyth and Nurse 1981). These cdc mutants elongate at the restrictive temperature and include mutants blocked at specific points throughout the cell cycle (Nurse *et al.* 1976). However, no mutants in this collection are blocked at the mitosis-to-interphase transition, perhaps because this is not a stage in the cell cycle during which cell elongation normally occurs (Nurse *et al.* 1976).

In a pilot screen to isolate mutants blocked at the mitosis-to-interphase transition, without making presuppositions regarding their cellular morphology, a bank of temperature-sensitive lethal mutants was screened for the ability to complete a normal mitosis but not to enter S phase at the restrictive temperature. Completion of mitosis was determined by the microscopic examination of cells stained with the DNA fluorochrome 4′,6′-diamino-2-phenylindole (DAPI) to identify binucleated cells with apparently equal amounts of DNA in the two daughter cells. To determine whether the mutants arrested before initiating S phase, the DNA content was measured by flow cytometry. One mutant, now called pim1-d1^{ts}, has these two characteristics indicative of a cell cycle arrest between the completion of mitosis and the initiation of S phase, and it also has highly condensed chromosomes (Sazer and Nurse 1994). In pim1-d1^{ts}, other aspects of progression from mitosis to interphase proceed normally, including a decline in the p34^{cdc2} kinase activity, a reorganization of the microtubules from the nuclear mitotic spindle apparatus to the cytoplasmic microtubule network, and the formation of a medial septum (Sazer and Nurse 1994). Subsequent analysis has revealed that the pim1-d1^{ts} cells undergo nuclear envelope fragmentation at the restrictive temperature, although the nuclear envelope normally re-

Corresponding author: Shelley Sazer, Verna and Marrs McLean Department of Biochemistry, Baylor College of Medicine, One Baylor Plaza, Houston, TX 77030. E-mail: ssazer@bcm.tmc.edu

mains intact throughout mitosis in yeast (Demeter *et al.* 1995), and that the medial septum increases in width the longer cells are incubated at the restrictive temperature (Matynia *et al.* 1996).

The pim1-d1^{ts} mutant is defective in pim1, the guanine nucleotide exchange factor (GEF) for spi1, a GTPase that was isolated as a high-copy suppressor of temperature-sensitive pim1 mutants (Matsumoto and Beach 1991; Sazer and Nurse 1994). In fission yeast, the genes encoding the third core component of the GTPase switch system, rna1, the GTPase-activating protein (GAP), and sbp1, a coactivator of the GAP, have recently been identified and characterized (Melchior *et al.* 1993; Bischoff *et al.* 1995; Matynia *et al.* 1996; He *et al.* 1998). The characteristic terminal phenotype of pim1-d1^{ts} cells, harboring a temperature-sensitive loss-of-function mutation in the GEF, is shared with cells in which either rna1 or sbp1 is depleted or overproduced (Matynia *et al.* 1996; He *et al.* 1998). These observations led to the hypothesis that an imbalance between the GDP- and GTP-bound forms of spi1 interferes with the ability of cells to reestablish the interphase state after mitosis (He *et al.* 1998; Matynia *et al.* 1996). pim1, spi1, rna1, and sbp1 are evolutionarily conserved proteins, homologs of which are known to influence a variety of biological processes *in vivo* and *in vitro*. Among these are nucleocytoplasmic transport of RNA and protein, cell cycle progression, and nuclear envelope structure, suggesting that the GTPase may have multiple downstream targets (reviewed in Dasso 1995; Sazer 1996).

Having identified and characterized the pim1-d1^{ts} mutant, it is now possible to use information about its terminal phenotype to isolate additional mutants defective in the mitosis-to-interphase transition. Because altering the ratio of the nucleotide-bound forms of the spi1 GTPase results in a characteristic terminal phenotype, this phenotype can be used as an identifying feature of new mutants that are defective in the spi1 GTPase system. Characterization of such mutants may lead to the identification of other components of the pathway that regulate the spi1 GTPase system or link it to downstream targets that influence the morphological and regulatory processes required for the mitosis-to-interphase transition. We report here the results of a screen to identify a class of fission yeast mutants that are unable to properly reestablish the interphase state after mitosis, based primarily on two easily identifiable morphological characteristics of the pim1-d1^{ts} strain: a wide medial septum and postmitotic chromosomes with abnormal states of condensation.

We have isolated a collection of 17 sns (septated, not in S-phase) mutants that fall into 14 complementation groups. Three of these mutants are allelic with pim1-d1^{ts}. sns mutants in 11 of the other 13 complementation groups show genetic interactions with *spi1*$^+$, *pim1*$^+$, *rna1*$^+$, and/or *sbp1*$^+$, and they are likely to identify regulators or targets of the spi1 GTPase pathway.

MATERIALS AND METHODS

Yeast strains and cell culture: All strains were derived from the wild-type haploid strain 972 h^- (Leupold 1970). Cells were grown at 25° (permissive temperature) and arrested by shifting to 36° (restrictive temperature) for 4 hr. Cell cycle synchronization was performed by nitrogen starvation (Sazer and Nurse 1994). Standard methods were used to perform matings and to isolate diploid strains based on intragenic complementation between two different *ade6* mutations (Moreno *et al.* 1991). The diploid strains were tested for sporulation ability by iodine staining and by random spore analysis. In cases where standard methods did not result in the isolation of stable diploids, nonsporulating diploids were generated with the *mat2-B102* mutation (Egel 1973). Identification of temperature-sensitive colonies was performed by replica plating to yeast extract (YE) containing the vital dye phloxine B (Sigma, St. Louis). Additional *pim1*^{ts} mutants used were JD59, JD60, JD61, JD62, JDX571 (J. Demeter and S. Sazer, unpublished results), slg51 (K. Gould, personal communication), BG4C7, BG1B1 (B. Grallert, personal communication), ptr2 (Azad *et al.* 1997), and pim1-46^{ts} (Matsumoto and Beach 1991).

Flow cytometry: Cells were fixed in ethanol, and flow cytometry was performed using a flow cytometer (model XL-MCL; Coulter Electronics, Hialeah, FL) as described previously (Sazer and Nurse 1994). Cell sorting was performed using a Coulter Epics Model 753 flow cytometer with the Cicero Data Acquisition System (Cytomation, Fort Collins, CO). Aggregated samples were either sonicated or briefly digested for 4 min at room temperature in 1 mg/mL Novozym 234 (Interspex, Foster City, CA) and 0.3 mg/mL 100T zymolyase (Seikagaku America, Rockville, MD) to decrease cell clumping. Remaining cell aggregates were excluded from analysis by gating.

Mutagenesis: In screen A, 207,000 *leu1-32 ura4-D18 h*$^-$ cells were mutagenized with nitrosoguanidine to ~40% viability, and in screen B, 115,000 cells were mutagenized to 12% viability (Moreno *et al.* 1991). The cells were then grown at the permissive temperature of 25° and replica plated to 36° on YE phloxine B to facilitate identification of colonies enriched in dead cells. A total of 1204 temperature-sensitive colonies from screen A and 637 temperature-sensitive colonies from screen B were identified and screened microscopically for those enriched in septated cells. These 22 colonies were scraped from the plate and mounted in a fluorescent DNA-binding dye, DAPI (Sigma), and the DNA morphology was examined using an Axioskop fluorescence microscope (Carl Zeiss, Thornwood, NY). Nine mutants from screen A (sns-A1, sns-A2, sns-A3, sns-A4, sns-A5, sns-A6, sns-A8, sns-A10, and sns-A11) and eight mutants from screen B (sns-B1, sns-B2, sns-B3, sns-B4, sns-B5, sns-B6, sns-B7, and sns-B9) were selected for further characterization.

Synthetic lethality with *pim1-d1*: Haploid double mutants of pim1-d1^{ts} and each of the sns strains were isolated by tetrad dissection, streaked on YE plates, and incubated at 31°, a temperature at which all single mutants grew to colonies. Double mutants that were dead were categorized as having strong synthetic lethality. Decreased growth compared to the single mutants was categorized as weak synthetic lethality, and colony growth comparable to the single mutants was categorized as no synthetic lethality.

Rescue by and sensitivity to GTPase components: pREP3X-*spi1*$^+$ (Matynia *et al.* 1996), pREP3X-*pim1*$^+$ (Sazer and Nurse 1994), pREP3X-*rna1*$^+$ (Matynia *et al.* 1996), or pREP41X-*sbp1*$^+$ (He *et al.* 1998) under control of the regulatable *nmt1* promoter (Forsburg 1993; Maundrell 1990) were transformed into wild-type and sns strains by standard electroporation or lithium acetate protocols (Okazaki *et al.* 1990; Moreno

et al. 1991). Cells were plated on Edinburgh Minimal Media (EMM) plates with appropriate supplements and 5 μg/mL thiamine to repress the *nmt1* promoter. The transformed strains were then streaked to EMM plates at the permissive temperature with thiamine to repress or without thiamine to derepress expression of the cDNA. The strains with the promoter on were then restreaked to promoter-on conditions, and strains with the promoter off were restreaked to promoter-off conditions. Rescue was tested at 36°, whereas sensitivities were tested at a range of temperatures from 25° to 34°.

Microscopy: Live cells were stained with 3,3′-dihexyloxacarbocyanine iodide ($DiOC_6$; Molecular Probes, Eugene, OR) to visualize the nuclear envelope and with Hoechst 33342 (Sigma) to visualize the DNA (Demeter *et al.* 1995). DAPI was used to visualize DNA in fixed cells (Moreno *et al.* 1991). Cells were observed and photographed with a Zeiss Axioskop fluorescence microscope.

Sequencing: To determine the sequence of the *pim1*$^+$ gene in sns-A3, sns-A5, and sns-A6, the open reading frame corresponding to the *pim1*$^+$ cDNA (Sazer and Nurse 1994) was amplified by PCR in two overlapping segments using the following oligonucleotide primers: pair 1, GGGGCATATGAA AAATGGCAAAAATGGCAAAAAGCCGG and GGGGCATA TGCTAAGCAGTGG; pair 2, GCGTCTGGTGATGGTTGC and CGTAGTTTTCAGCAGATCC. The PCR products were directly sequenced using the CYCLIST exo$^-$ PFU kit (Stratagene, La Jolla, CA).

RESULTS

sns mutant isolation: Approximately 322,000 wild-type cells were mutagenized with nitrosoguanidine, grown at the permissive temperature of 25°, and replica plated to 36° on YE phloxine B to facilitate identification of the 1841 temperature-sensitive colonies. Each of these was examined microscopically by observing the cells at the edge of the colony to identify those with a high percentage of septated cells. Twenty-two colonies that were enriched for septated cells were identified. To determine that the temperature-sensitive arrest was not caused by chromosome separation defects, cells from each of these 22 colonies were scraped from the plate, mixed with DAPI in 50% glycerol, and observed by fluorescence microscopy. Seventeen strains arrested as septated, binucleated cells with an apparently equal distribution of chromosomes and abnormal states of chromosome condensation. These 17 strains were named sns-A1, sns-A2, sns-A3, sns-A4, sns-A5, sns-A6, sns-A8, sns-A10, sns-A11, sns-B1 sns-B2, sns-B3, sns-B4, sns-B5, sns-B6, sns-B7, and sns-B9. All of the strains were backcrossed three times to wild-type cells to ensure that a single mutation was responsible for the phenotype observed, and subsequent analyses were performed on these backcrossed strains.

Linkage and complementation analysis of sns mutants: To determine if the sns strains were mutated in the *pim1*$^+$ gene, each was crossed to the pim1-d1^{ts} mutant. Three strains, sns-A3, sns-A5, and sns-A6, had mutations that were tightly linked to pim1-d1^{ts}. Linkage analysis was then performed among the remaining 14 strains to determine how many independent genes are represented. No wild-type recombinants were found in a total of 1425 progeny by random spore analysis when sns-A10 was crossed to sns-A11, indicating that the mutations in these strains are tightly linked. Subsequent analyses revealed that they are mutated in the same gene (A. Matynia and S. Sazer, unpublished results). Therefore, further characterization was performed only on sns-A10, leaving 14 different mutants for further analysis. The other 12 sns strains were unlinked.

Heterozygous diploid strains were generated with each of the sns mutants and wild-type cells. All 17 sns strains were found to carry recessive mutations, based on the observation that the phenotype of these diploids at the restrictive temperature was wild type.

The ability of the genes mutated in the 13 non-*pim1*^{ts} sns strains to complement each other was tested. These 13 mutants were crossed pairwise, and diploid double mutants were isolated based on color selection for the *ade6-M210* and *ade6-M216* mutations. The diploid double mutants, sns-A1/sns-A4, sns-A2/sns-B5, sns-A4/sns-A8, sns-A4/sns-B2, and sns-A4/sns-B6, were isolated by generating nonsporulating diploid caused by the presence of the *mat2-B102* mutation (Egel 1973). The diploid double mutants exhibited no occurrences of unlinked noncomplementation because all strains were able to grow normally at the restrictive temperature.

Molecular characterization of new *pim1*^{ts} alleles: To determine whether sns-A3, sns-A5, and sns-A6 were indeed mutated in the *pim1*$^+$ gene, the *pim1*$^+$ gene was amplified from the genome of these mutants by PCR and sequenced. Similarly, the sequence of *pim1*$^+$ was determined for nine other temperature-sensitive mutants that were isolated in independent screens carried out in several laboratories, including our own, and were expected to be mutated in the *pim1*$^+$ gene based on linkage and/or phenotypic characterization. We also sequenced the *pim1-d1*^{ts} (Sazer and Nurse 1994) and *pim1-46*^{ts} (Matsumoto and Beach 1991) alleles. Figure 1A shows the position of the eight different amino acid changes that result from mutations in the *pim1*$^+$ gene in these 14 strains. The mutations map throughout the coding region, and all but one mutation lie in the evolutionarily conserved repeats. pim1-d1^{ts} and pim1-46^{ts} contain different mutations that map to repeats II and V, respectively. sns-A5 and sns-A6 contain the same mutation as pim1-46^{ts}, and sns-A3 is a new mutation. Therefore, one new allele was identified in the sns screen, and five new alleles were identified from other screens.

Phenotypic characterization of the *pim1*^{ts} mutants: Similar to the pim1-d1^{ts} and pim1-46^{ts} strains, the three *pim1*^{ts} sns strains and all the additional *pim1*^{ts} mutants, which were obtained from independent screens, were fully rescued by *pim1*$^+$. All of the *pim1*^{ts} strains were also fully rescued by overexpression of *spi1*$^+$, except for sns-A3, which was rescued only very weakly by *spi1*$^+$ overexpression (rescue of sns-A3 compared to JDX571 by *pim1*$^+$ and *spi1*$^+$ is shown in Figure 1B). The terminal pheno-

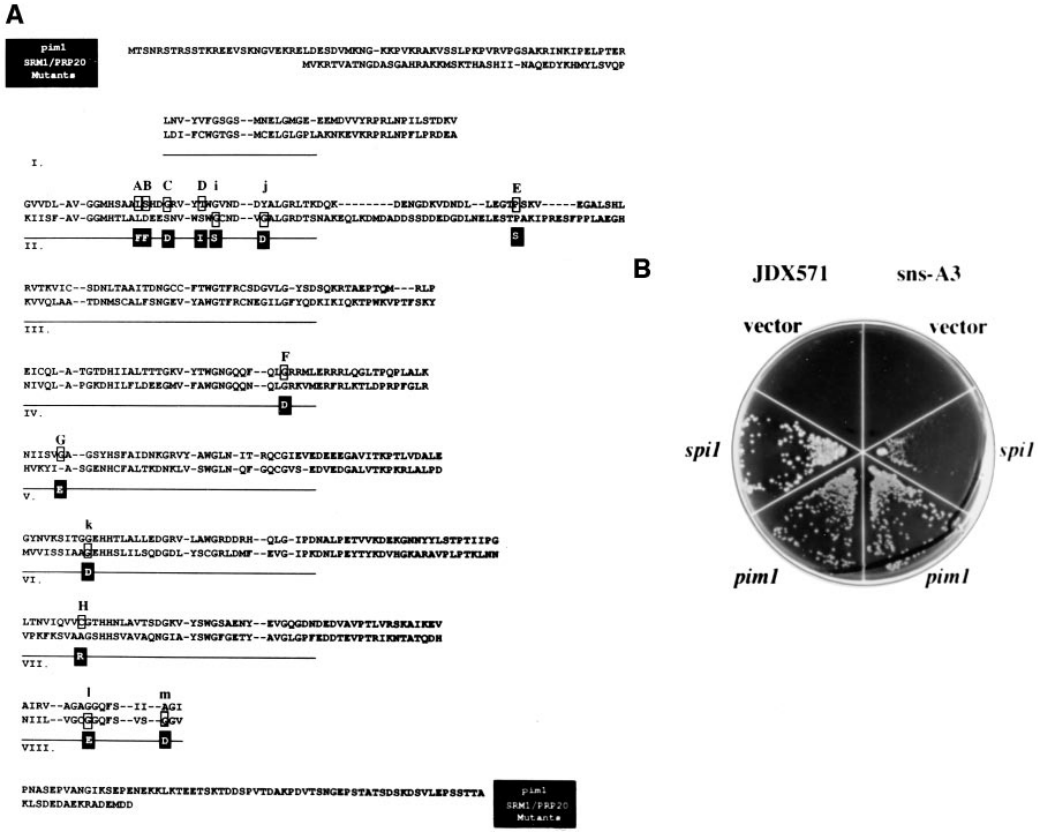

Figure 1.—Sequence of *pim1*^{ts} alleles and rescue of the pim1 mutants by *spi1*$^{+}$ and *pim1*$^{+}$. (A) *S. pombe* pim1 and *Saccaromyces cerevisiae* Prp20 protein sequences are aligned. The repeats, numbered I–VIII (Lee *et al.* 1994), are underlined. The locations of the mutations are indicated by open boxes. The amino acid changes are indicated in black boxes. *S. pombe* mutants are as follows: A, JD61; B, pim1-d1^{ts}; C, JD62 and ptr2; D, JD60, E, slg51; F, JD59; G, sns-A5, sns-A6, pim1-46^{ts}, and BG4C7; H, sns-A3. *S. cerevisiae* mutants are as follows: i, mtr1-2; j, srm1-1; k, mtr1-1; l, prp20-1; m, prp20-4 and mtr1-3. (B) JDX571 and sns-A3 were transformed with pREP41X, pREP3X-*spi1*$^{+}$, or pREP3X-*pim1*$^{+}$, and they were grown at the restrictive temperature. JDX571 is fully rescued by overexpression of *spi1*$^{+}$ or *pim1*$^{+}$ but not by the empty vector. sns-A3 is fully rescued by overexpression of *pim1*$^{+}$, weakly by *spi1*$^{+}$, and is not rescued by the empty vector.

type of these *pim1*^{ts} mutants was the same as that previously described for the pim1-d1^{ts} mutant: cells arrested with a wide medial septum, hypercondensed chromatin, and fragmented nuclear envelopes. As has been demonstrated previously for the *pim1-46* allele (Matsumoto and Beach 1993), Western blot analysis showed the pim1 protein level decreased in all these mutants after 4 hr at the restrictive temperature (data not shown).

Phenotypic characterization of the non-*pim1*^{ts} sns mutants: Each of the 13 non-*pim1*^{ts} sns strains was analyzed for DNA content, septation index, DNA morphology, and nuclear envelope phenotypes. These strains all arrested at the restrictive temperature as septated, binucleated cells with an apparently equal amount of DNA in each daughter cell and a septation index >25% (Table 1). *Schizocaccaromyces pombe* cells in G1 have a 1C DNA content per nucleus, but the daughter cells have not yet separated (Sazer and Nurse 1994). Therefore, septated cells in G1 have a 2C DNA content, whereas binucleated cells that have replicated their DNA in the cell cycle without completing cytokinesis have a 4C DNA content.

TABLE 1

Phenotypic analysis of sns strains

Strain	DNA condensation	Nuclear envelope	Percent septated
sns-A1	Moderate	Normal	37
sns-A2	Moderate	Normal	35
sns-A3	Hyper	Abnormal	45
sns-A4	Moderate	Normal	31
sns-A5	Hyper	Abnormal	40
sns-A6	Hyper	Abnormal	51
sns-A8	Hypo	Normal	80
sns-A10	Hyper	Abnormal	34
sns-B1	Hypo	Normal	32
sns-B2	Hyper	Normal	36
sns-B3	Hypo	Normal	35
sns-B4	Hypo	Normal	33
sns-B5	Hypo	Normal	31
sns-B6	Moderate	Normal	46
sns-B7	Moderate	Normal	49
sns-B9	Moderate	Abnormal	27

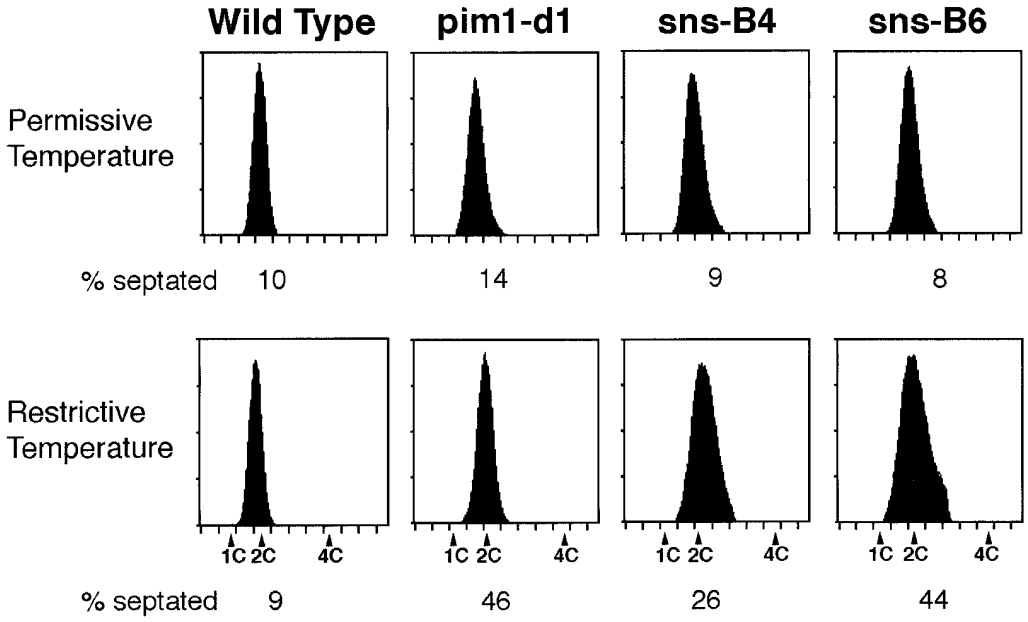

Figure 2.—DNA content of the sns strains at the restrictive temperature. Mutant strains were grown at the permissive or restrictive temperature and analyzed by flow cytometry. The percentage of septated cells in each sample is indicated. Wild type, pim1-d1, and two examples of the sns mutants, sns-B4 and sns-B6, have a 2C DNA content at both the permissive and restrictive temperatures. Because the mutants accumulate binucleated cells, their 2C total DNA content demonstrates that they have a 1C DNA content per nucleus.

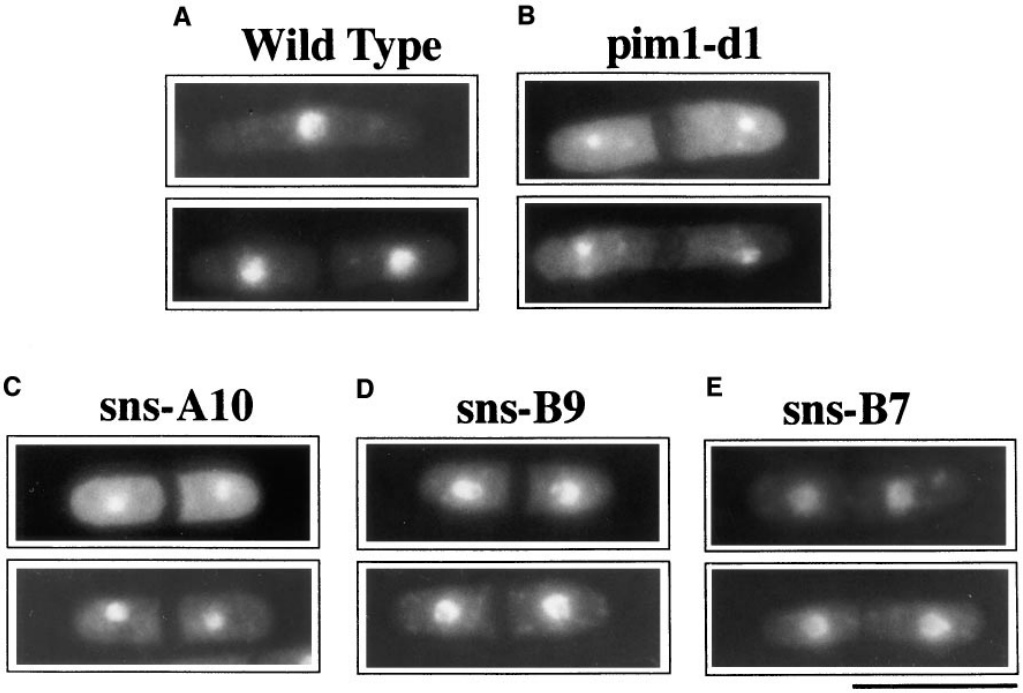

Figure 3.—DNA morphology of the sns strains at the restrictive temperature. Wild-type or mutant cells at the restrictive temperature were stained with DAPI to visualize the DNA. Two representative cells are shown for each strain. (A) Wild-type cells show the normal interphase state of decondensed DNA. (B) pim1-d1^{ts} cells show hypercondensed DNA. (C) sns-A10 has hypercondensed DNA. (D) sns-B9 has moderately condensed DNA. (E) sns-B7 has hypocondensed DNA. Bar, 10 μm.

The sns strains all arrest with a 2C DNA content, as measured by FACS analysis, indicating that the arrested binucleate cells have a 1C DNA content per nucleus (wild type, pim1-d1, sns-B4, and sns-B6 shown in Figure 2). sns-A8 also arrests with a 1C DNA content per nucleus as either binucleated, septated cells with a 2C total DNA content or as a four-cell filament with a 4C total DNA content. The identity of the sns-A8 cells in the 2C and 4C peaks was verified by microscopic examination of cells sorted on the basis of DNA content (data not shown). Examination of the DNA morphology was carried out using DAPI. Examples of the varying states of DNA condensation observed in the sns mutants are shown in Figure 3. Wild-type cells with decondensed DNA (Figure 3A) and pim1-d1^{ts} cells with hypercondensed DNA (Figure 3B) are shown for comparison. sns-A10 and sns-B2 have hypercondensed DNA, similar to the pim1-d1^{ts} strain (sns-A10 is shown in Figure 3C). sns-A1, sns-A2, sns-A4, sns-B6, and sns-B9 have moderately condensed DNA (sns-B9 is shown in Figure 3D). sns-A8, sns-B1, sns-B3, sns-B4, sns-B5, and sns-B7 have hypocondensed DNA, which appears less densely packed than wild-type interphase DNA (sns-B7 is shown in Figure 3E). The DNA morphology of these 13 sns mutants is summarized in Table 1.

Further phenotypic characterization of live sns mutant cells was performed using $DiOC_6$, a general membrane dye, to delineate the nuclear envelope, and Hoechst, a DNA-binding dye, to indicate the position of the nucleus. Examples of normal and abnormal nuclear envelopes in the sns mutants are shown in Figure 4. pim1-d1^{ts} cells at the permissive temperature with normal nuclear envelopes (arrows in Figure 4, A and B) and at the restrictive temperature with abnormal nuclear envelopes (septated cells indicated by arrowheads in Figure 4, C and D) that are known to be fragmented (Demeter *et al.* 1995) are shown for comparison. At the restrictive temperature, the nuclear envelopes appear abnormal, no longer forming a visible circular ring surrounding the DNA, in sns-A10 and sns-B9 (septated sns-A10 cells, indicated by arrowheads, are shown in Figure 4, E and F). However, nuclear envelopes appear normal, completely encircling the DNA in sns-A1, sns-A2, sns-A4, sns-A8, sns-B1, sns-B2, sns-B3, sns-B4, sns-B5, sns-B6, and sns-B7 (a septated sns-A2 cell, indicated by the arrowhead, is shown in Figure 4, G and H). The nuclear envelope morphology of the sns strains is summarized in Table 1.

Synthetic lethality of sns mutants with pim1-d1^{ts}: To identify mutant strains that interact genetically with the spi1 GTPase system, haploid double mutants were made with pim1-d1^{ts} and each of the 13 sns strains. Growth of the double mutants was compared to each of the two single mutants at the permissive temperature of 31°, a temperature at which pim1-d1^{ts} and the single sns mutants grew normally. The genes mutated in four strains, sns-A1, sns-A2, sns-A8, and sns-B2, showed a strong synthetic lethality with *pim1-d1* (Figure 5A). The genes mutated in six additional strains, sns-A4, sns-A10, sns-B1, sns-B4, sns-B7, and sns-B9, showed weak synthetic lethality with *pim1-d1* (Figure 5, B and C). The genes mutated in the remaining strains, sns-B3, sns-B5 and sns-B6, showed no synthetic lethality with *pim1-d1* (Figure 5D). The results of these synthetic lethality tests are summarized in Table 2.

Epistasis analysis of pim1-sns double mutants: To determine if the genes mutated in the non-*pim1*^{ts} sns strains act upstream or downstream of *pim1*$^{+}$, each of the haploid pim1-sns double mutants was arrested at 36°, and the chromatin and nuclear envelopes were examined using either DAPI or Hoechst and $DiOC_6$. Because all of the single mutants are septated when arrested, the degree of chromatin condensation and the condition of the nuclear envelope were used to clearly distinguish the mutant phenotypes. Because the phenotypes of pim1-d1 and sns-A10 are indistinguishable at this level, sns-A10 was excluded from epistasis analysis. Eight of the double mutants, pim1sns-A1, pim1sns-A4, pim1sns-B1, pim1sns-B3, pim1sns-B5, pim1sns-B6, pim1sns-B7, and pim1sns-B9, arrested with hypercondensed DNA and abnormal nuclear envelopes, which are characteristics of the pim1-d1 phenotype. pim1sns-A2 arrested with moderately condensed DNA and normal nuclear envelopes, which corresponds to the sns-A2 phenotype. Because the double mutants pim1sns-A8, pim1sns-B2, and pim1sns-B4 grew poorly in minimal media, these strains were grown and shifted to the restrictive temperature in a rich medium, YE. Examination of their DNA and nuclear envelope morphology revealed that all three of these strains arrested with the pim1-d1 phenotype under these conditions.

Rescue of sns mutants by components of the spi1 GTPase system: To further test for genetic interactions of the sns mutants with the spi1 GTPase system, rescue by overexpression of the four known components of the GTPase system (*spi1*$^{+}$, *pim1*$^{+}$, *rna1*$^{+}$, and *sbp1*$^{+}$) was assayed. Rescue of the sns strains by a known component of the GTPase system would indicate either that the strain is mutated in that protein or that the GTPase component is a high-copy suppressor of the sns mutant, much like *spi1*$^{+}$ is a high-copy suppressor of pim1-d1^{ts}. The 13 sns strains were transformed with plasmids containing cDNA inserts encoding the known GTPase components, *spi1*$^{+}$, *pim1*$^{+}$, *rna1*$^{+}$, or *sbp1*$^{+}$, whose transcription was driven by the thiamine-regulatable *nmt1* promoter at sublethal levels. sns-B3 could not be transformed by standard techniques and was therefore excluded from these analyses. Strains sns-A1, sns-A8, sns-B4, and sns-B5 showed a thiamine-dependent growth defect and were excluded from these analyses. The growth of the remaining sns strains at 36° under promoter-on conditions was compared to promoter-off conditions. None of the sns strains were rescued by *spi1*$^{+}$, *pim1*$^{+}$, *rna1*$^{+}$, or *sbp1*$^{+}$ (data not shown).

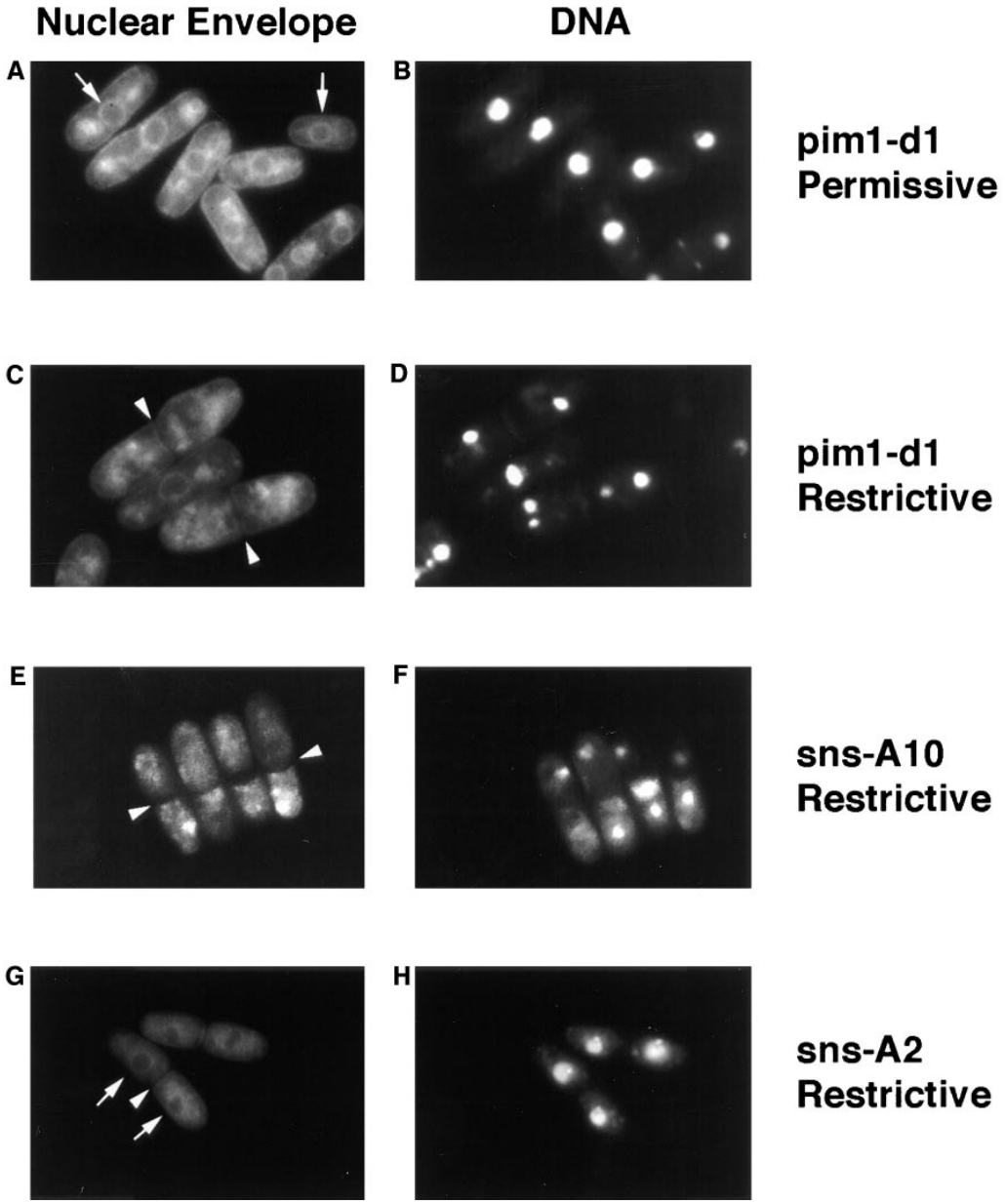

Figure 4.—Nuclear envelope morphology of sns strains. Mutant cells at the permissive or restrictive temperature were stained with $DiOC_6$ to delineate the nuclear envelope (A, C, E, and G) and with Hoechst to indicate the position of the nucleus (B, D, F, and H). Septated cells are indicated by arrowheads, and normal nuclear envelopes are indicated by arrows. (A and B) pim1-d1^{ts} cells at the permissive temperature have normal nuclear envelopes that encircle the DNA. (C and D) pim1-d1^{ts} cells at the restrictive temperature have abnormal nuclear envelopes that do not surround the DNA. (E and F) sns-A10 cells at the restrictive temperature have abnormal nuclear envelopes that do not encircle the DNA. (G and H) sns-A2 cells at the restrictive temperature have normal nuclear envelopes that encircle the DNA.

Sensitivity of sns mutants to overexpression of the GTPase components: Loss of function of the GEF in the pim1-d1^{ts}strain at a semipermissive temperature coupled to overexpression of either the GAP, rna1, or its coactivator, sbp1, results in a dramatic decrease in viability (Matynia *et al.* 1996; He *et al.* 1998). This is presumably because the expected increase in the proportion of spi1-GDP resulting from the GEF mutation and overexpression of either the GAP or its coactivator are additive. sns strains that are mutated in regulators or targets of the spi1 GTPase are likely to have an imbalance in the nucleotide-bound state of spi1 and, therefore, should also be sensitive to overexpression of any of the GTPase components that exacerbate this imbalance.

Wild-type cells grow normally when *spi1*$^+$ is overexpressed from the strongest *nmt1* promoter, pREP3X (Sazer and Nurse 1994), but they are sensitive to overexpression of *pim1*$^+$ and *rna1*$^+$ from this promoter; they have reduced viability but still form colonies (Sazer and Nurse 1994; Matynia *et al.* 1996). Wild-type cells,

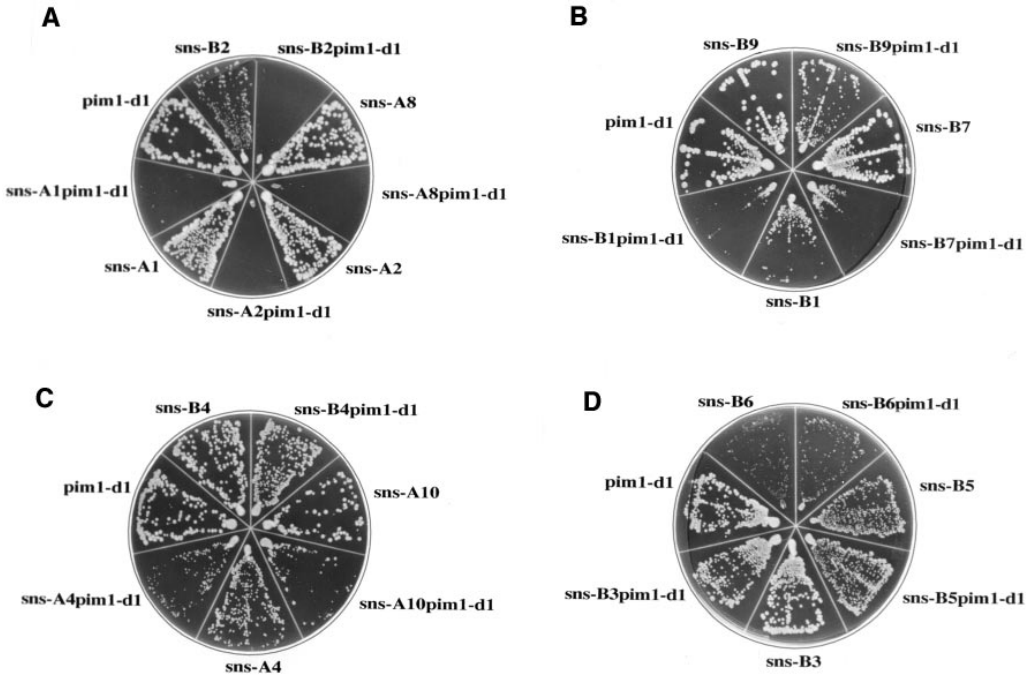

Figure 5.—Synthetic lethality of the sns strains with pim1-d1^{ts}. Haploid double mutant cells and the single mutants from which they were generated were streaked at the semipermissive temperature of 31°. (A) sns-A1, sns-A2, sns-A8, and sns-B2 show a strong synthetic lethality with pim1-d1^{ts}. (B and C) sns-A4, sns-A10, sns-B1, sns-B4, sns-B7, and sns-B9 show a weak synthetic interaction. (D) sns-B3, sns-B5, and sns-B6 show no synthetic lethality.

however, exhibit lethality upon *sbp1*$^+$ overexpression using the strongest *nmt1* promoter (He *et al.* 1998). *sbp1*$^+$ was therefore overexpressed from the medium-strength *nmt1* promoter in the pREP41X plasmid to achieve an expression level that is not toxic to wild-type cells.

The growth of wild-type and sns strains containing either pREP3X-*spi1*$^+$, pREP3X-*pim1*$^+$, pREP3X-*rna1*$^+$, or pREP41X-*sbp1*$^+$ under promoter-on or promoter-off conditions was compared (Figure 6). sns-B3 could not be transformed by standard techniques and was therefore excluded from these analyses. Furthermore, strains sns-A1, sns-A8, sns-B4, and sns-B5 showed a thiamine-sensitive growth defect and were excluded from these analyses. The other sns strains were grown at a range of temperatures from 29° to 34° because the temperature sensitivities of these strains vary. Results for strains that were sensitive to *spi1*$^+$, *pim1*$^+$, *rna1*$^+$, or *sbp1*$^+$ overexpression are shown for the lowest temperature at which a sensitivity was detected (Figure 6, A–D).

Three strains, sns-A2, sns-B1, and sns-B9, showed strong sensitivity, and sns-B6 showed a weaker but significant sensitivity to overexpression of the spi1 GTPase (Figure 6A). Five strains, sns-A2, sns-A4, sns-A10, sns-B1, and sns-B6, showed sensitivity to *pim1*$^+$ overexpression (Figure 6B). sns-A10 and sns-B1 showed strong sensitivity to *pim1*$^+$ overexpression, whereas the other three strains showed weak-to-moderate sensitivity. Six strains, sns-A2, sns-A4, sns-A10, sns-B1, sns-B6, and sns-B9, showed a strong sensitivity to *rna1*$^+$ overexpression (Figure 6C). Five of the 13 strains, sns-A2, sns-A10, sns-B1, sns-B6, and sns-B9 showed sensitivity to *sbp1*$^+$ overexpression (Figure 6D). sns-A10 and sns-B9, showed a strong sensitivity to *pim1*$^+$ overexpression, whereas the other three strains showed a weak-to-moderate sensitivity. Results of the four sensitivity tests, which are indicative of a genetic interaction between the sns mutants and the spi1 GTPase system, are summarized in Table 3.

DISCUSSION

The septated phenotype of pim1-d1^{ts}, the prototypic mitosis to interphase mutant in fission yeast, was used

TABLE 2

Synthetic lethality of the sns strains with the pim1-dl^{ts} strain

Strain	Synthetic lethality with pim 1-dl
sns-A1	Strong
sns-A2	Strong
sns-A4	Weak
sns-A8	Strong
sns-A10	Weak
sns-B1	Weak
sns-B2	Strong
sns-B3	None
sns-B4	Weak
sns-B5	None
sns-B6	None
sns-B7	Weak
sns-B9	Weak

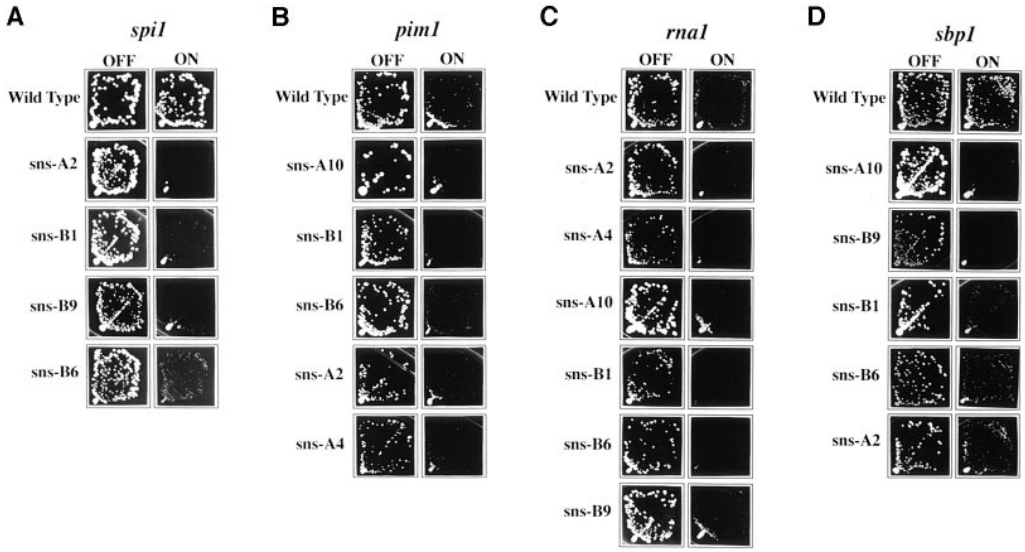

Figure 6.—Sensitivity of the sns strains to overexpression of known spi1 GTPase components. sns strains containing pREP3X-*spi1*$^+$, pREP3X-*pim1*$^+$, pREP3X-*rna1*$^+$, or pREP41X-*sbp1*$^+$ driven by the thiamine-repressible *nmt1* promoter were grown under promoter-off and promoter-on conditions. Sensitivity to overexpression of the different GTPase components was assessed as impaired growth as compared to wild-type cells. Photographs of the sns strains are presented in decreasing order of sensitivity. (A) sns-A2, sns-B1, sns-B9, and sns-B6 overexpressing *spi1*$^+$ show growth sensitivity. (B) sns-A10, sns-B1, sns-B6, sns-A2, and sns-A4 overexpressing *pim1*$^+$ show growth sensitivity. (C) sns-A2, sns-A4, sns-A10, sns-B1, sns-B6, and sns-B9 overexpressing *rna1*$^+$ show growth sensitivity. (D) sns-A10, sns-B9, sns-B1, sns-B6, and sns-A2 overexpressing *sbp1*$^+$ show growth sensitivity. sns strains not shown exhibited no sensitivity to overexpression of *spi1*$^+$, *pim1*$^+$, *rna1*$^+$, or *sbp1*$^+$, or they exhibited a thiamine-dependent growth defect and could not be assessed by this test. sns-A2, sns-A4, and sns-B1 sensitivities were tested at 29°, wild-type, sns-A10, and sns-B6 were tested at 32°, and sns-B9 was tested at 34°.

as the basis for a larger scale screen. We report here the initial characterization of 17 temperature-sensitive mutant strains that, like the pim1-d1^{ts} mutant, are blocked at the transition from mitosis to interphase.

TABLE 3

Sensitivity of the sns strains to overexpression of known spi1 GTPase components

Strain	*spi1*$^+$ sensitivity	*pim1*$^+$ sensitivity	*rna1*$^+$ sensitivity	*sbp1*$^+$ sensitivity
sns-A2	Strong	Weak	Strong	Weak
sns-A4	None	Weak	Strong	None
sns-A10	None	Strong	Strong	Strong
sns-B1	Strong	Strong	Strong	Weak
sns-B2	None	None	None	None
sns-B6	Weak	Weak	Strong	Weak
sns-B7	None	None	None	None
sns-B9	Strong	None	Strong	Strong
sns-A1[a]	ND	ND	ND	ND
sns-A8[a]	ND	ND	ND	ND
sns-B3[b]	ND	ND	ND	ND
sns-B4[a]	ND	ND	ND	ND
sns-B5[a]	ND	ND	ND	ND

ND, not determined.

[a] Strains sns-A1, sns-A8, sns-B4, and sns-B5 displayed a thiamine-dependent growth defect and are therefore not included in these analyses.

[b] Strain sns-B3 could not be transformed by standard methods and is therefore not included in these analyses.

These 17 sns strains were identified and selected for further study based on DNA morphology and content and on septation index. sns-A10 and sns-A11 were tightly linked, and subsequent analysis showed that they were mutated in the same gene. In addition, sns-A3, sns-A5, and sns-A6 were found to be allelic with pim1-d1^{ts}. Therefore, the screen identified 14 different genes that, when mutated, result in an inability to reestablish the interphase state. *pim1*^{ts} mutants were isolated three times, a second mutant was isolated twice, and all other sns mutants are represented by a single allele. This indicates that the screen is not yet saturated.

Three sns mutants are allelic with pim1-d1^{ts}: Sequencing of the *pim1*$^+$ gene from sns-A3, sns-A5, and sns-A6, the original pim1-d1^{ts} and pim1-46^{ts} strains, as well as nine additional alleles isolated in independent screens, identified eight different mutations that result in amino acid substitutions located throughout the pim1 protein. The pim1 protein and its homologs, the mammalian RCC1 and the budding yeast Prp20/Srm1/Mtr1, have an internal repeat structure in which an imperfectly conserved domain is repeated fully six times and partially twice (Ohtsubo *et al.* 1989; Aebi *et al.* 1990; Lee *et al.* 1994). Despite this repeat structure, which is the only identifiable motif, the protein family has several known biochemical activities: it binds the GTPase (Bischoff and Ponstingl 1991; Matsumoto and Beach 1993), catalyzes nucleotide exchange on the GTPase (Bischoff and Ponstingl 1991), associates with chro-

matin (Seino *et al.* 1992; Lee *et al.* 1993), and binds double-stranded DNA in vitro (Ohtsubo *et al.* 1989; Lee *et al.* 1993). *In vitro* kinetic studies of mutant GEF proteins, whose charged amino acids were converted to alanine, suggest that specific conserved histidines (the 13th amino acid of the repeat, Figure 1A) are important for the exchange reaction and that the C-terminal half of the repeats are important for binding the GTPase (Azuma *et al.* 1996). Based on observations in budding yeast, it has been suggested that the different repeats of the GEF protein may perform separate functions. First, strains carrying mutations in the seventh and eighth repeats, but not in the second and third repeats, could be rescued by overexpression of the GTPase (Kadowaki *et al.* 1993; Lee *et al.* 1994). Second, proteins with mutations in the second and third repeat retained their *in vitro* double-stranded DNA-binding activity, but those with mutations in the eighth repeat lost this activity (Lee *et al.* 1994).

In the case of *pim1*$^+$, we have characterized 14 mutants that represent eight different alleles. All of the mutants were rescued by *spi1*$^+$ overexpression, including strains carrying mutations in the nonconserved spacer between repeats two and three, and in the second repeat. In the *S. cerevisiae* homolog, mutations in the second repeat are not rescued by overproduction of the GTPase. The mutation in sns-A3 maps to the seventh repeat and is only weakly rescued by *spi1*$^+$ overexpression. In the *S. cerevisiae* homolog, however, mutations in the seventh repeat are rescued by overproduction of the GTPase. These observations suggest that the structural organization of the GEF is more complex than expected. With the recent solution of the three-dimensional structure of the mammalian GEF (L. Renault and A. Wittinghofer, personal communication), a better understanding of its structure-function relationship is now possible.

The eight *pim1*^{ts} mutants described in this manuscript were isolated in several independent screens, but they all arrest with a medial septum and condensed chromosomes, and they are rescued by overproduction of the spi1 GTPase. Although there is a substantial decrease in the level of pim1 protein in all these mutants at the restrictive temperature, they do not behave as null mutants that cannot be rescued by spi1 overproduction (Matsumoto and Beach 1991). Because the terminal pim1-like phenotype upon which the isolation of the sns mutants was based was not a criterion in the screens that identified the BG1B1, BG4C7, slg51, ptr2, JD59, JD60, JD61, JD62, or JDX571 mutants, it is significant that no separation of function mutations in *pim1*$^+$ were identified among this collection.

Phenotypic characterization of the 14 non-*pim1*^{ts} sns mutants representing 13 complementation groups: Phenotypic characterization was performed on the 13 sns strains that were not alleles of *pim1*$^+$. All 13 sns strains were arrested at the restrictive temperature after nuclear division as septated cells that have not entered S phase. However, the sns strains differ in their state of chromatin condensation and their nuclear envelope morphology (summarized in Table 1). The mutant strains have varying degrees of DNA condensation from hypercondensed to hypocondensed DNA. The level of DNA condensation does not appear to directly correspond with abnormalities in the nuclear envelopes because mutants were found that have highly condensed DNA and normal nuclear envelopes (*e.g.*, sns-B2) or that have only moderately condensed DNA and abnormal nuclear envelopes (*e.g.*, sns-B9). The differences in these mutants and the fact that these DNA and nuclear envelope phenotypes are independent may be useful in elucidating the sequential steps that are required at the mitosis-to-interphase transition. Additionally, they may aid in understanding the primary defect caused by perturbations in the spi1 GTPase system by delineating specific steps or targets in this pathway.

Ten of the non-*pim1*^{ts} sns strains are synthetically lethal with *pim1-d1*^{ts}: Genetic interactions with the spi1 GTPase system were assayed by determining whether the genes that are mutated in any of the sns strains were synthetically lethal with *pim1-d1*. There was a strong synthetic lethality between *pim1-d1* and the genes mutated in sns-A1, sns-A2, sns-A8, and sns-B2. The genes mutated in these strains are therefore likely to be in the spi1 GTPase pathway. The genes mutated in six other strains showed a weak synthetic lethality and are therefore less definite in their placement in the spi1 GTPase pathway. The genes mutated in the remaining three strains showed no synthetic lethality and are therefore unlikely to be in the spi1 GTPase pathway, but they may represent components of an independent pathway required for mitotic exit.

The non-*pim1*^{ts} sns strains are not rescued by overexpression of the known components of the spi1 GTPase system: To determine which of the sns strains are likely to have mutations in components of the spi1 GTPase pathway and which may have mutations in proteins that influence mitotic exit independently, further genetic analyses were performed. Each mutant was transformed with *spi1*$^+$, *pim1*$^+$, *rna1*$^+$, or *sbp1*$^+$ to determine if it could be rescued by overexpression of these known components of the GTPase system. *spi1*$^+$ overexpression rescues pim1-d1^{ts} and pim1-46^{ts}, but it does not rescue a deletion of *pim1*$^+$, indicating that it is not a bypass suppressor (Matsumoto and Beach 1991; Sazer and Nurse 1994). This type of genetic relationship suggested that pim1 and spi1 interact physically, a prediction that has subsequently been demonstrated biochemically (Bischoff and Ponstingl 1991). The three *pim1*^{ts} mutant strains identified in this screen, sns-A3, sns-A5, and sns-A6, were also rescued by *spi1*$^+$. None of the other 13 sns strains showed high-copy suppression by *spi1*$^+$, *pim1*$^+$, *rna1*$^+$, or *sbp1*$^+$ and are therefore not likely to be mutated in these genes. They may, however, be

mutated in previously unidentified components of the spi1 GTPase system.

Eleven of the non-*pim1*^{ts} sns mutants are hypersensitive to overexpression of known components of the spi1 GTPase system: Previous studies have indicated that a precise balance between the GTP- and GDP-bound forms of spi1 is the essential feature of this GTPase system required for normal cell cycle progression (Matynia *et al.* 1996). Consistent with this hypothesis is the fact that cells are unable to complete the mitosis-to-interphase transition when spi1 would be expected to accumulate in either the GDP- or GTP-bound form (Matynia *et al.* 1996; He *et al.* 1998). Based on this model, the level of *spi1*$^+$ expression would not be expected to have an effect on cell cycle progression as long as the nucleotide-bound state of spi1 was regulated properly. However, four strains, sns-A2, sns-B1, sns-B6, and sns-B9, showed sensitivity to overexpression of *spi1*$^+$. These four mutants are particularly intriguing because they may localize spi1 improperly or have an imbalance in the nucleotide-bound state of spi1 that is exacerbated when *spi1*$^+$ is overexpressed. Additionally, these sns strains showed sensitivity to *pim1*$^+$, *rna1*$^+$, and *sbp1*$^+$ overexpression, which is consistent with a defect in the localization or regulation of spi1.

In contrast to *spi1*$^+$ overexpression, *pim1*$^+$, *rna1*$^+$, or *sbp1*$^+$ overexpression is expected to directly alter the nucleotide-bound state of spi1. spi1 would accumulate in the GTP-bound form upon *pim1*$^+$ overexpression or upon loss of rna1 or sbp1. Alternatively, spi1 is expected to accumulate in the GDP-bound form upon *rna1*$^+$ or *sbp1*$^+$ overexpression, or upon a loss of pim1, as in the pim1-d1^{ts} strain. The effects of a mutation in *pim1*$^+$ and overexpression of *rna1*$^+$ or *sbp1*$^+$ are additive (Matynia *et al.* 1996; He *et al.* 1998). When *rna1*$^+$ or *sbp1*$^+$ is overexpressed in pim1-d1^{ts} cells grown at a semipermissive temperature, the viability is severely reduced and the pim1 phenotype is more penetrant. sns strains that exhibit sensitivity to overexpression of *pim1*$^+$ may represent genes that are mutated in unknown regulators of spi1 that normally enhance the hydrolysis of GTP by spi1. Similarly, sns strains that exhibit sensitivity to overexpression of *rna1*$^+$ or *sbp1*$^+$ may represent genes that are mutated in unknown regulators of spi1 that normally enhance the rate of GDP to GTP exchange. No sns strains were found to be sensitive only to *pim1*$^+$ or only to *rna1*$^+$ and *sbp1*$^+$ overexpression. The genes mutated in the sns strains are therefore unlikely to be mutated in upstream regulators of the spi1 GTPase system.

sns-A4 was unique in that it showed sensitivity to *rna1* overexpression but not to *sbp1*$^+$ overexpression, which increases the GAP activity of rna1 *in vitro* (Bischoff *et al.* 1995). The identification of this mutant, which is sensitive to an increase in the GAP activity brought about by an increase in GAP protein level but not by an increase in the level of its coactivator, suggests that sbp1 may have additional functions and that sns-A4 may be useful in delineating them.

Five strains, sns-A2, sns-A4, sns-A10, sns-B1, and sns-B6, showed a sensitivity to *pim1*$^+$ overexpression as well as a strong sensitivity to *rna1*$^+$ overexpression. The same strains, excluding sns-A4, showed sensitivity to *sbp1*$^+$ overexpression. Sensitivity to overexpression of the GEF, the GAP, and the GAP coactivator indicates that these strains are sensitive to the accumulation of either spi1-GDP or spi1-GTP, suggesting that the genes mutated in these strains are likely to act downstream of the spi1 GTPase.

pim1-d1 is epistatic to nine of the sns mutants: To determine which of the genes mutated in the sns strains act upstream or downstream of *pim1*$^+$, the DNA and nuclear envelope morphology of the pim1-sns double mutants was examined. For the sns strains that show a genetic interaction with pim1-d1, the results of this analysis would place the sns gene action either upstream or downstream in a *pim1*$^+$-dependent pathway (Hartwell *et al.* 1974). For the sns strains that did not show genetic interaction, this analysis would place the sns gene action chronologically, in an independent pathway.

Eleven sns strains, sns-A1, sns-A2, sns-A4, sns-A8, sns-A10, sns-B1, sns-B2, sns-B4, sns-B6, sns-B7, and sns-B9, are likely to be in the *pim1*$^+$ pathway, based on synthetic lethality and overexpression hypersensitivity. Consistent with these analyses, the pim1-d1 double mutants of these sns strains arrest with the mutant phenotype of one of the single mutants. The double mutants pim1sns-A1, pim1sns-A4, pim1sns-A8, pim1sns-B1, pim1sns-B2, pim1sns-B4, pim1-sns-B6, pim1sns-B7, and pim1sns-B9 arrest with hypercondensed chromatin and abnormal nuclear envelopes, as does pim1-d1. The genes mutated in these strains are therefore likely to act downstream of *pim1*$^+$, in a dependent pathway. However, pim1sns-A2 arrested with the DNA and nuclear envelope morphology of sns-A2, indicating that the gene mutated in sns-A2 is likely to act upstream of *pim1*$^+$. The overexpression sensitivity assays indicated that this gene may effect the localization or regulation of spi1. It is therefore possible that this gene represents a new regulator of *spi1*$^+$. The DNA and nuclear envelope phenotypes of sns-A10 are similar to pim1-d1, thereby precluding epistasis analysis for the pim1sns-A10 double mutant.

Neither sns-B3 nor sns-B5 showed any genetic interactions with the spi1 GTPase system and are therefore likely to be mutated in genes required in a spi1-independent pathway for the mitosis-to-interphase transition. Because both pim1sns-B3 and pim1sns-B5 arrested with the pim1-d1 DNA and nuclear envelope morphology, it is most probable that the execution points of the genes mutated in sns-B3 and sns-B5 occur after the action of *pim1*$^+$ in an independent pathway.

Summary: Seventeen mutant sns strains that represent 14 complementation groups defective at the mitosis-to-interphase transition have been identified in *S. pombe*.

Three sns mutants are defective in pim1, the previously characterized GEF for the spi1 GTPase. The 14 non-*pim1*^{ts} sns strains fall into 13 complementation groups. Two of the non-*pim1*^{ts} sns strains, sns-B3 and sns-B5, do not show genetic interactions with the spi1 GTPase system and may identify independent functions required for the mitosis-to-interphase transition. Eleven of the 13 non-*pim1*^{ts} sns mutants are likely to be mutated in new components of the spi1 GTPase system because they showed genetic interactions with the known components of the GTPase system. Epistasis analysis of the pim1-sns double mutants places the action of the genes mutated in nine of these 11 strains downstream of *pim1*$^{+}$ and one upstream of *pim1*$^{+}$. Two strains, sns-B1 and sns-B6, are likely to be mutated in genes that act downstream of *pim1*$^{+}$, based on both overexpression hypersensitivity and epistasis analyses. These analyses also indicate that sns-A2 is likely to be mutated in a gene that acts upstream of *pim1*$^{+}$. Another strain, sns-A4, may help identify potential multiple roles of sbp1, the GAP coactivator. sns-A10 is also likely to be mutated in a gene that acts downstream of *pim1*$^{+}$, based on overexpression hypersensitivity analysis, although epistasis analysis could not be performed because of indistinguishable phenotypes. Seven other strains, sns-A1, sns-A8, sns-B2, sns-B4, sns-B7, and sns-B9, exhibited genetic interactions with the spi1 GTPase system in at least one test performed and, based on epistasis analysis, are likely to act downstream of *pim1*$^{+}$. These sns strains will therefore be useful for identifying both the upstream regulators and downstream targets of the spi1 GTPase, thereby elucidating the primary role(s) of this GTPase system *in vivo* and delineating the steps required for the reestablishment of the interphase state after mitosis.

The authors thank S. Salus, K. Dimitrov, and U. Fleig for critical reading of the manuscript; K. Gould, B. Grallert, Y. Ohshima, D. Beach, and T. Matsumoto for providing pim1 mutant strains. We also thank X. He and P. Logan for assistance in the preliminary characterization of the sns mutants and D. Lewis, W. Schobe, and J. Scott for assistance with the FACS analysis. This research was supported by grants to S.S. from the National Institutes of Health (GM 49119) and the Human Frontier Science Program (RG423/95M). A.L.G. was supported by a National Science Foundation REU Site Grant (B10-9200400), and K.H. was supported by a Robert A. Welch Foundation Undergraduate Scholarship (Q1226).

LITERATURE CITED

Aebi, M., M. W. Clark, U. Vijayraghavan and J. Abelson, 1990 A yeast mutant, *PRP20*, altered in mRNA metabolism and maintenance of the nuclear structure, is defective in a gene homologous to the human gene *RCC1* which is involved in the control of chromosome condensation. Mol. Gen. Genet. **224:** 72–80.

Azad, A. K., T. Tokio, N. Shiki, S. Tsuneyoshi, S. Urushiyama *et al.*, 1997 Isolation and molecular characterization of mRNA transport mutants in *Schizosaccharomyces pombe*. Mol. Biol. Cell **8:** 825–841.

Azuma, Y., H. Seino, T. Seki, S. Uzawa, C. Klebe *et al.*, 1996 Conserved histidine residues of RCC1 are essential for nucleotide exchange on Ran. J. Biochem. **120:** 82–91.

Bischoff, F. R., and H. Ponstingl, 1991a Catalysis of guanine nucleotide exchange on Ran by the mitotic regulator RCC1. Nature **354:** 80–82.

Bischoff, F. R., and H. Ponstingl, 1991b Mitotic regulator protein RCC1 is complexed with a nuclear ras-related polypeptide. Proc. Natl. Acad. Sci. USA **88:** 10830–10834.

Bischoff, F. R., H. Krebber, T. Kempf, I. Hermes and H. Ponstingl, 1995 Human RanGTPase-activating protein RanGAP1 is a homologue of yeast Rna1p involved in mRNA processing and transport. Proc. Natl. Acad. Sci. USA **92:** 1749–1753.

Dasso, M., 1995 The role of the Ran GTPase pathway in cell cycle control and interphase nuclear functions, pp. 163–172 in *Progress in Cell Cycle Research*, edited by L. Meijer, S. Guidet and H. Y. L. Tung. Plenum Press, New York.

Demeter, J., M. Morphew and S. Sazer, 1995 A mutation in the RCC1-related protein pim1 results in nuclear envelope fragmentation in fission yeast. Proc. Natl. Acad. Sci. USA **92:** 1436–1440.

Egel, R., 1973 Commitment to meiosis in fission yeast. Mol. Gen. Genet. **121:** 277–284.

Forsburg, S. L., 1993 Comparison of *Schizosaccharomyces pombe* expression systems. Nucleic Acids Res. **21:** 2955–2966.

Hagan, I. M., and J. S. Hyams, 1988 The use of cell division cycle mutants to investigate the control of microtubule distribution in the fission yeast *Schizosaccharomyces pombe*. J. Cell Sci. **89:** 343–357.

Hartwell, L. H., J. Culotti, J. R. Pringle and B. J. Reid, 1974 Genetic control of the cell division cycle in yeast. Science **183:** 46–51.

He, X., N. Naoyuki, N. G. Walcott, Y. Azuma, T. E. Patterson *et al.*, 1998 The identification of cDNAs that affect the mitosis-to-interphase transition in *Scizosaccharomyces pombe*, including *sbp1*, which encodes a spi1p-GTP binding protein. Genetics **148:** 645–656.

Kadowaki, T., D. Goldfarb, L. M. Spitz, A. M. Tartakoff and M. Ohno, 1993 Regulation of RNA processing and transport by a nuclear guanine nucleotide release protein and members of the Ras superfamily. EMBO J. **12:** 2929–2937.

Lee, A., R. Tam, P. Belhumeur, T. DiPaolo and M. W. Clark, 1993 Prp20, the *Saccharomyces cerevisiae* homolog of the regulator of chromosome condensation, RCC1, interacts with double-stranded DNA through a multi-component complex containing GTP-binding proteins. J. Cell Sci. **106:** 287–298.

Lee, A., K. L. Clark, M. Fleischmann, M. Aebi and M. W. Clark, 1994 Site-directed mutagenesis of the yeast *PRP20/SRM1* gene reveals distinct activity domains in the protein product. Mol. Gen. Genet. **245:** 32–44.

Leupold, U., 1970 Genetic methods for *Schizosaccharomyces pombe*. Meth. Cell Physiol. **4:** 169–177.

Matsumoto, T., and D. Beach, 1991 Premature initiation of mitosis in yeast lacking RCC1 or an interacting GTPase. Cell **66:** 347–360.

Matsumoto, T., and D. Beach, 1993 Interaction of the pim1/spi1 mitotic checkpoint with a protein phosphatase. Mol. Biol. Cell **4:** 337–345.

Matynia, A., K. Dimitrov, U. Mueller, X. He and S. Sazer, 1996 Perturbations in the spi1p GTPase cycle of *Schizosaccharomyces pombe* through its GTPase-activating protein and guanine nucleotide exchange factor components result in similar phenotypic consequences. Mol. Cell. Biol. **16:** 6352–6362.

Maundrell, K., 1990 nmt1 of fission yeast. J. Biol. Chem. **265:** 10857–10864.

Melchior, F., K. Weber and V. Gerke, 1993 A functional homologue of the *RNA*1 gene product in *Schizosaccharomyces pombe:* purification, biochemical characterization, and identification of a leucine-rich repeat motif. Mol. Biol. Cell **4:** 569–581.

Moreno, S., A. Klar and P. Nurse, 1991 Molecular genetic analysis of fission yeast *Schizosaccharomyces pombe*. Methods Enzymol. **194:** 795–823.

Murray, A., and T. Hunt, 1993 *The Cell Cycle: An Introduction*. W. H. Freeman, New York.

Nasmyth, K., and P. Nurse, 1981 Cell division cycle mutants altered in DNA replication and mitosis in the fission yeast *Scizosaccharomyces pombe*. Mol. Gen. Genet. **182:** 119–124.

Nurse, P., 1975 Genetic control of cell size at cell division in yeast. Nature **256:** 547–551.

Nurse, P., P. Thuriaux and K. Nasmyth, 1976 Genetic control of the cell division cycle in the fission yeast *Schizosaccharomyces pombe*. Mol. Gen. Genet. **146:** 167–178.

Ohtsubo, M., H. Okazaki and T. Nishimoto, 1989 The RCC1 pro-

tein, a regulator for the onset of chromosome condensation locates in the nucleus and binds to DNA. J. Cell Biol. **109:** 1389–1397.

Okazaki, K., N. Okazaki, K. Kume, S. Jinno, K. Tanaka *et al.*, 1990 High-frequency transformation method and library transducing vectors for cloning mammalian cDNAs by trans-complementation of *Schizosaccharomyces pombe*. Nucleic Acids Res. **18:** 6485–6489.

Robinow, C. F., and J. S. Hyams, 1989 General cytology of fission yeast, pp. 273–324 in *Molecular Biology of Fission Yeast*, edited by A. Nasim, P. Young and B. F. Johnson. Academic Press, San Diego.

Sazer, S., 1996 The search for the primary function of the Ran-GTPase continues. Trends Cell Biol. **6:** 81–85.

Sazer, S., and P. Nurse, 1994 A fission yeast RCC1-related protein is required for the mitosis to interphase transition. EMBO J. **13:** 606–615.

Seino, H., N. Hisamoto, S. Uzawa, T. Sekiguchi and T. Nishimoto, 1992 DNA-binding domain of RCC1 protein is not essential for coupling mitosis with DNA replication. J. Cell Sci. **102:** 393–400.

Communicating editor: M. D. Rose